# Theoretical Study of CO Adsorption on Gold/Alumina Substrates

**Eva M. Fernández* and Luis C. Balbás**

*Departamento de Física Teórica, Atómica y Óptica, Universidad de Valladolid, E-47011 Valladolid, Spain*

*Received: January 20, 2006; In Final Form: March 27, 2006*

Aiming to understand the role of the substrate in the adsorption of carbon monoxide on gold clusters supported on metal-oxides, we have started a study of that process on two different alumina substrates: an amorphous-like fully relaxed stoichiometric $(Al_2O_3)_{20}$ cluster and the Al terminated (0001) surface of $\alpha$-$(Al_2O_3)$ crystal. In this paper, we present first principles calculations for the adsorption of one Au atom on both alumina substrate and the adsorption of $Au_8$ on $(Al_2O_3)_{20}$. Then, we study the CO adsorption on the minimum energy structure of these three different gold/alumina systems. A single Au adsorbs preferably on top of an Al atom with low coordination, the binding energy being higher in the case of $Au/(Al_2O_3)_{20}$. CO absorbs preferably on top of the Au atom, but in the case of $Au/(Al_2O_3)_{20}$, Au forms a bridge with the Al and O substrate atoms after CO adsorption. We find other stable sites for CO adsorption on the cluster but not on the surface. This result suggests that the Au activity toward CO may be larger for the amorphous cluster than for the crystal surface substrate. For the most stable $Au_8/(Al_2O_3)_{20}$ configuration, two Au atoms bind to Al and a O atoms respectively and CO adsorbs on top of the Au which binds to the Al atom. We find other CO adsorption sites on supported $Au_8$ which are not stable for the free $Au_8$ cluster.

## Introduction

The interface of a gold-cluster/metal-oxide is being intensively studied at present due to their surprisingly high catalytic activity toward the oxidation of carbon monoxide.[1] It has been found also that the metal-oxide interface has important industrial applications, such as heterogeneous catalysis[2] or microelectronics.[3] The roll of the metal-oxide support in these applications is an important issue. There are many factors that influence the reactivity of a cluster/oxide system. Heiz and co-workers[4,5] found that the catalytic activity for the CO oxidation of Au clusters supported on MgO shows a strong dependence on the size and charge state of the cluster. Wörz et al.[6] found that if the metal is oxidized previously it is more active. Schübert and co-workers[7] found different activity for Au clusters on different substrates, for example, an irreducible oxide such as $Al_2O_3$ and MgO, or reducible oxide, such as $Fe_2O_3$ and $TiO_2$. Recently, it has been shown[8] that gold/$TiO_2$ and gold/$Al_2O_3$ are the most active catalysts for CO oxidation. The activity of a metal/support system can also change when the size of the support is reduced to the nanometric scale.[9,10]

In the literature, there are a large number of experimental and theoretical studies on aluminum oxide films $Al_2O_3$ and an increasing amount of experimental work on the Au/alumina interface,[7−9,11,12] but very few of these concern the theoretical aspects of that interface. Cruz-Hernández and Fernández-Sanz[13] have considered the adsorption of atomic gold on the unreconstructed Al terminated (0001) surface of $\alpha$-$Al_2O_3$, resulting a maximum adsorption energy of 0.81 eV for Au on top of a surface oxygen (pertaining to the second surface layer). Feng and co-workers[14] reported Au(111)/$Al_2O_3$ interface calculations using three different models for the $\alpha$-alumina termination, namely, Al, O, and 2 Al layers, and two types of commensurate (111)/(0001) strained interfaces, concluding that only the Al-terminated interfaces can be observed.

* Corresponding author. Tel.: +34 983 42 31 44. Fax: +34 983 42 30 13. E-mail: eva@lcb.fam.cie.uva.es.

To study the effect of the shape and size of the oxide support on the CO adsorption on Au/alumina complexes, in this work, we perform first a density functional theory (DFT) study of the most favorable adsorption site of the Au atom on two different alumina substrates: an amorphouslike $(Al_2O_3)_{20}$ cluster and the $\alpha$-$Al_2O_3$ (0001) corundum surface. Second, we calculate the binding energy for adsorption of CO at equilibrium positions on both Au/alumina substrates. Finally, we present the calculated optimal configuration for $Au_8$ adsorption on the alumina cluster and the subsequent study of CO adsorption on the $Au_8/(Al_2O_3)_{20}$ system. We compare our results for Au on alumina with related previous calcuations.[13] To shed light on the substrate effects, we are going to compare our results for CO/$Au_8$/alumina with those for CO adsorption on a free $Au_n$ cluster studied by us in a previous work.[15]

## Computational Methods

The electronic calculations are performed using the first principles code SIESTA (Spanish initiative for electronic simulation of thousands of atoms).[16] The electronic structure is described within the spin dependent generalized gradient approximation (GGA) for the exchange-correlation potential.[17] We use standard norm-conserving pseudopotentials.[18] They were generated with the atomic valence-electron configuration $2s^2$-$2p^2$ for C, $2s^22p^4$ for O, $3s^23p^1$ for Al and $5d^{10}6s^1$ for Au. Flexible linear combinations of numerical (pseudo)atomic orbitals are used as the basic set, allowing for multiple-$\xi$ and polarization orbitals. To limit the range of the basic pseudo-atomic orbitals (PAO), they are slightly excited by a common "energy shift" (here, we take 0.005 Ry for O and Al and 0.001 Ry for C) and truncated at the resulting radial node. In the present calculation, we use a double-$\xi$ s,p-basis and single d for C, O, and Al, and double-$\xi$ s,d-basis and single p polarization orbital for Au. The basis functions and the electron density are projected onto a uniform real space grid in order to calculate the Hartree and exchange correlation potentials and matrix

10.1021/jp060426l CCC: $33.50 
Published on Web 05/10/2006

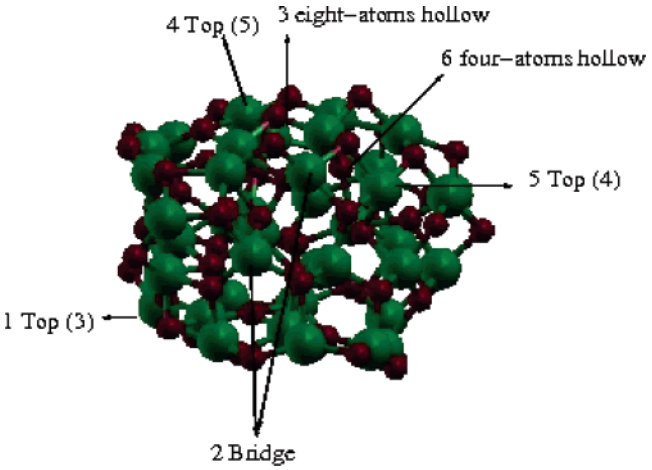


**Figure 1.** Equilibrium geometry of $(Al_2O_3)_{20}$ amorphouslike cluster determined in ref 19. All the atoms were fully relaxed up to forces smaller than 0.015 eV/Å. The adsorption sites of atomic gold are shown and numbered from the larger to the smaller binding energies. The number in parentheses indicates the coordination number of the substrate atom.

elements. The grid fineness is controlled by the "energy cutoff" of the plane waves that can be represented in it without aliasing (here we take 120 Ry). The geometry was optimized within the conjugate-gradient method until the force on each atom was smaller than 0.015 eV/Å. We test several different initial positions for the adsorbed molecule. For the adsorption on the (0001) corundum surface calculations, we have considered a 2 × 2 unit cell with nine layers and we fully relaxed the first six layers, maintaining the other three as fixed.[19] In ref 19, we performed a study of the (0001) surface relaxation for several numbers of layers and multiplicity of the unit cell. Good agreement with other state of the art calculations was obtained for a 1 × 1 cell with 15 and 21 layers. In this work, we take a 2 × 2 unit cell with nine layers as a compromise among accurate results and very consuming time calculations. Other tests concerning the basis and pseudopotentials used here within the Siesta method have been presented in previous papers about alumina clusters[20] and gold clusters.[21]

## Results and Discussion

**Au Adsorption.** The initial geometries of both alumina substrates, the $(Al_2O_3)_{20}$ cluster and the Al-terminated (0001) surface of α-$(Al_2O_3)$ were characterized in a previous work.[19] The structure of $(Al_2O_3)_{20}$ was obtained by determining self-consistently the minimum energy structures of $(Al_2O_3)_n$ clusters,[20] starting with $n = 1$ and adding units of $Al_2O_3$ one by one up to $n = 20$, and it is represented in Figure 1. Analyzing the distribution of Al−O pair distances and the partial density of states (PDOS) of that structure, we conclude in ref 19 that this cluster structure resembles amorphous alumina oxide. For the corundum (0001) model, we take here the result of ref 19 corresponding to a 2 × 2 unit cell with nine layers having the first six layers fully relaxed. In this model, the $d_{i,i+1}$ interlayer separations are −97.4%, 8.4%, −29.6%, and 26.0% for $i = 1-4$, measured in percent with respect to the $d_{i,i+1}$ of the bulk crystal in the (0001) direction. First, we study an Au adatom on both substrates testing different initial positions. The adsorption energy of a gold cluster on the alumina substrate is calculated as

$$E_{ads} = E[Au_n] + E[(Al_2O_3)_{substrate}] - E[Au_n/(Al_2O_3)_{substrate}]$$

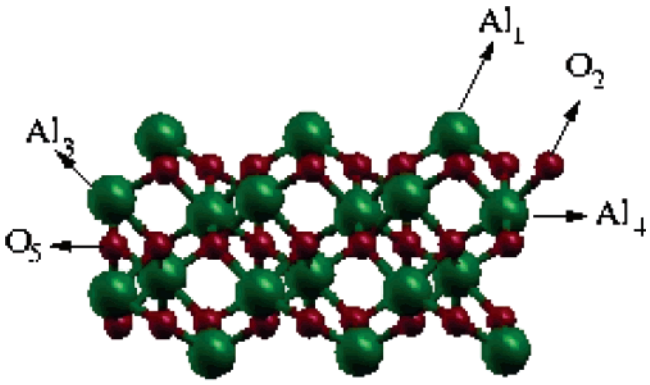


**Figure 2.** Initial adsorption site of the Au adatom on the Al-terminated α-alumina (0001) surface. The subindexes indicate the atom layer where the Au is adsorbed.

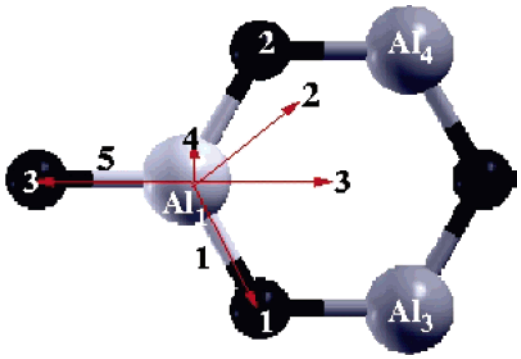


**Figure 3.** Equilibrium adsorption positions of Au on the α-alumina surface.

where $(Al_2O_3)_{substrate}$ stands for $(Al_2O_3)_{20}$ or α-$Al_2O_3$ (0001) and $E[X]$ is the total energy of system X in the minimum energy local equilibrium configuration.

For the α-$Al_2O_3$ (0001) substrate, we consider initially the Au atom in different positions: on top of Al of the first, third, and fourth layer; on top of O of the second and fifth layer. Sites on the Al of the third and fourth layer, and on O of the fifth layer, actually are hollow sites in which Au binds three surface oxygen atoms. These positions are shown in Figure 2. All these cases evolve after relaxation to equilibrium adsorption sites with Au bound to Al in the first surface layer. In Figure 3 are represented schematically these Au adsorption sites, whose electronic and geometrical preoperties are characterized in Table 1. The binding energy difference of these isomers is due to the different environment of the Au adtom with respect to the surface (angles $\alpha_1$ and $\alpha_2$). Positions 1, 2, and 3 correspond, in first approximation, to three points in a circle parallel to the second oxygen layer formed by $O_1$, $O_2$, and $O_3$ (see Figure 3) with the center vertically on the Al of the first layer. The Au−$Al_1$ distance is 2.54−2.59 Å, and the difference in the adsorption energy is due to the proximity of the Al of the third and fourth layer. We guess that the barriers for the Au hopping among the sites of that circle are small. On the other hand, adatom site 4 is near vertical to the surface ($\alpha_3 \approx 90°$), and site 5 is less favorable energetically than site 3 because Au competes with $O_3$ for the electrons of $Al_1$.

After adsorption, the surface atoms closer to Au are displaced. This effect is made apparent by a displacement of ∼0.39−0.48 Å in the $z$ direction of the Al atoms where the Au binds (the lateral displacement are very small, ≤0.03 Å) and a contraction in the angles $\alpha_{O-Al-O} \sim 5.3°-8.8°$. The other Al atoms of the first layer are slightly displaced down the surface or do not change at all (remember that we are using a 2 × 2 unit cell).

**TABLE 1: Properties of Au Atoms Adsorbed on Different Sites (see Figure 3) of an α-$Al_2O_3$ (0001) Surface**

| | $E_{ads}$[a] (eV) | $d_{Au-Al_1}$[b] (Å) | $\Delta Q_{Au}$[b] (\|e\|) | $\alpha_1$[d] | $\alpha_2$[d] | $\alpha_3$[e] | $\Delta_{Al-O}$[f] | $\Delta\alpha_{OAlO}$[g] | $\Delta z$[h] |
|---|---|---|---|---|---|---|---|---|---|
| 1 | 0.78 | 2.54 | 0.12 | 70.0° | 114.4° | 52.2° | 0.06 | −8.9° | 0.46 |
| 2 | 0.77 | 2.55 | 0.14 | 103.5° | 73.0° | 51.4° | 0.05 | −8.0° | 0.46 |
| 3 | 0.76 | 2.59 | 0.14 | 85.1° | 81.° | 44.8° | 0.03 | −6.1° | 0.48 |
| 4 | 0.72 | 2.53 | 0.14 | 105.4° | 103.5° | 88.3° | 0.02 | −5.3° | 0.39 |
| 5 | 0.52 | 2.54 | 0.12 | 123.5° | 115.1° | 64.2° | 0.06 | −8.8° | 0.45 |

[a] Adsorption energy. [b] Distance Au−substrate. [c] Excess electronic charge on Au atom. [d] The term $\alpha_1$ is the angle formed by the line Au−$Al_1$ and $Al_1$−$O_1$ in Figure 2, and $\alpha_2$ is the angle formed by the lines Au−$Al_1$ and $Al_1$−$O_2$. [e] The term $\alpha_3$ is the angle formed by the line Au−$Al_1$ and the plane formed by $O_1$, $O_2$, and $O_3$. Changes of the substrate after Au adsorption are given for the properties in footnotes f and g. [f] The $Al_1$−O distance (Å). [g] The angle O−$Al_1$−O. [h] Increase of the $z$ coordinate (Å) of $Al_1$ in the first alumina layer.

**TABLE 2: Properties of Au Adsorbed on an $(Al_2O_3)_{20}$ Cluster[a]**

| | adsorption site[b] | $E_{ads}$ (eV) | $d$[c] (Å) | $\Delta Q_{Au}$ (\|e\|) |
|---|---|---|---|---|
| 1 | top Al (3) | 0.96 | 2.54 | 0.17 |
| 2 | bridge | 0.77 | 2.71−2.97 | 0.09 |
| 3 | eight-atom hollow | 0.76 | ⟨2.78⟩ | 0.06 |
| 4 | top Al (5) | 0.67 | 2.62 | 0.13 |
| 5 | top Al (4) | 0.54 | 2.67 | 0.13 |
| 6 | four-atom hollow | 0.36 | ⟨2.90⟩ | 0.02 |

[a] The first column identifies the position as in Figure 1. [b] See Figure 1. The coordination of the substrate atom is given in parentheses. [b] Distance Au−substrate. The symbol ⟨·⟩ denotes the average values for the first neighbor atoms.

This result disagrees with the one reported in ref 13 where the more favorable adsorption site is obtained on top of a subsurface O atom ($O_2$ in Figure 2), with a binding energy 0.81 eV and distance Au−O of 1.99 Å. In our calculation, the Al of the substrate is displaced 0.46 Å upward after binding the Au atom, that is, up to only 42,5% of the $d_{12}$ distance in the (0001) direction of the corundum crystal. Instead, in ref 13, the O atom of the substrate is displaced upward by 0.27 Å. These differences can be due to details of the calculations. The plane wave GGA calculation in ref 13 was performed for a 1 × 1 unit cell 12 layers thick, allowing structural relaxations of the six outermost layers until the residual forces on the atoms are less than 0.1 eV/Å. In our GGA calculation, we relax the six outermost layers of a 2 × 2 unit cell nine layers thick, which prevents Au−Au interaction, until the forces on the atoms are smaller than 0.015 eV/Å. However, when we allow forces as large as 0.1 eV/Å, all the tested initial Au adsorption sites remain practically unaltered after optimization, and all of them have similar adsorption energies ∼0.75 eV.

The $(Al_2O_3)_{20}$ cluster presents a greater variety of adatom initial positions than α-$Al_2O_3$ (0001) because of the amorphous structure and the larger number of Al and O surface atoms with different coordination numbers. The equilibrium adsorption sites of Au on $(Al_2O_3)_{20}$ clusters are shown in Figure 1 and are characterized in Table 2.

The adatom site on the $(Al_2O_3)_{20}$ with the higher binding energy is on top of one of the 3-fold coordinated Al surface atoms. We can see in Table 2 that the smaller Au-substrate distance (2.54 Å) corresponds to the larger adsorption energy (0.96 eV) and charge transfer (0.17 e). After adsorption, only the position and charge of the substrate atoms which are closer to the adatom are affected. This justifies, as a good approximation, fixing the positions of substrate atoms beyond the second neighbors of Au atoms, as we will do for the study of $Au_8$ adsorption on $(Al_2O_3)_{20}$ clusters.

The adsorption site of a single Au atom on both, cluster and surface substrates, is a 3-fold coordinated Al. However, the bond direction Au−Al for the higher binding energy configuration of Au/$(Al_2O_3)_{20}$ is perpendicular to the plane of the three O atoms which binds the Al atom. This site is similar to site 4 of Table 1 for the Au/surface system. Both, binding energy and excess charge, are about 20% larger for the Au/cluster than for Au/(0001) surfaces in their respective ground states, but the bond distance is similar for both systems. Analogous sites to 1, 3, 4, and 5 of Table 2 and Figure 3 can be defined initially for the α-alumina (0001) surface (sites 2 and 6 are found only in the cluster), but only site 1 is found for the equilibrium Au adatom on the surface, as commented above. From this point of view, considering only binding energy and adsorption sites, a cluster is more advantageous than a surface in forming Au/alumina substrates.

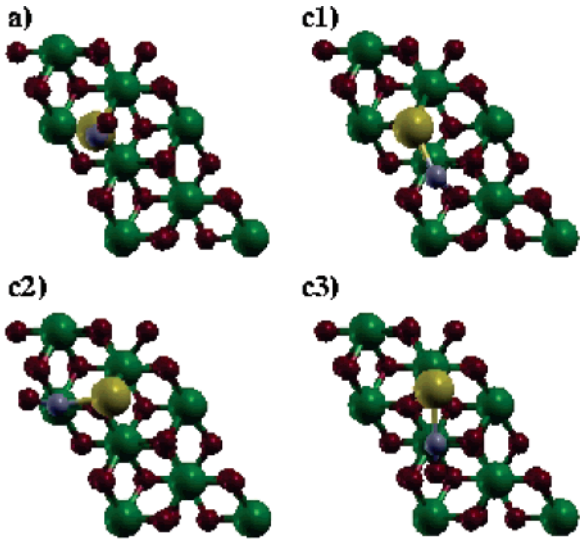


**Figure 4.** Higher adsorption energy sites of CO on the Au/α-$Al_2O_3$ substrate reported in Table 3. These show a portion of the surface.

**CO Adsorption.** To study the adsorption of CO on both Au/alumina substrates optimized in the preceding paragraphs, we consider the respective ground states for several different initial positions of CO binding to the Au adsorbed on 3-fold coordinated Al atoms. Then, we relax all the positions of atoms in the complexes, except the three deepest layers of the α-$Al_2O_3$ (0001) surface. The adsorption energy of CO is obtained as

$$E_{ads} = E[\mathrm{CO}] + E[\mathrm{Au}_n/(\mathrm{Al_2O_3})_{substrate}] - E[\mathrm{CO/Au}_n/(\mathrm{Al_2O_3})_{substrate}]$$

The equilibrium configurations after CO adsorption may occur directly on the Au atoms or at the interface of Au−substrate. In the first case, the effect on the configuration of the substrate is small. The equilibrium adsorption geometries on both Au/alumina substrates are represented in Figures 4 and 5, and in Table 3 are given the corresponding binding energies, charge transfer, and geometrical characterization.

For both substrates, the adsorption site with higher CO binding energy has the CO bond only to the Au atom. In the cluster case, after CO adsorption, the Au adatom is displaced

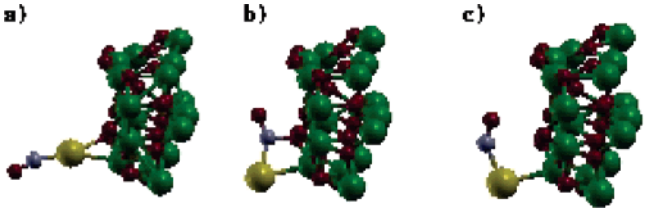


**Figure 5.** Higher adsorption energy sites of CO on the Au/$(Al_2O_3)_{20}$ substrate reported in Table 3. Only the relevant portion of the cluster is shown.

**TABLE 3: Properties of CO Adsorbed on an Au/$(Al_2O_3)_{20}$ Cluster and on an Au/α-$Al_2O_3$ Surface[a]**

| | site | $E_{ads}$ | $d_{CO}$ | $d_{CAu}$ | $\alpha_{AuCO}$[b] | $\alpha_{CAuAl}$[b] | $\Delta Q_c$[c] | $\Delta Q_O$[c] |
|---|---|---|---|---|---|---|---|---|
| $(Al_2O_3)_{20}$ | a | 1.05 | 1.18 | 1.95 | 160.5° | 152.2° | 0.12 | −0.18 |
| | b | 0.74 | 1.22 | 2.21 | 140.3° | 71.7° | 0.23 | −0.08 |
| | c | 0.64 | 1.17 | 2.07 | 145.1° | 99.3° | 0.12 | −0.25 |
| α-$Al_2O_3$ | a | 0.98 | 1.18 | 1.96 | 145.2° | 138.0° | 0.16 | −0.17 |
| | c1 | 0.78 | 1.17 | 2.05 | 140.1° | 126.1° | 0.19 | −0.23 |
| | c2 | 0.75 | 1.17 | 2.05 | 141.8° | 115.6° | 0.18 | −0.26 |
| | c3 | 0.75 | 1.17 | 2.05 | 136.3° | 107.5° | 0.17 | −0.28 |

[a] Notation for sites as in Figures 4 and 5. [b] Angles Au−C−O and C−Au−Al. [c] Excess of electronic charge (in |e|) on the C and O atoms of CO.

to form a Al−Au−O bridge with the alumina cluster and the Au−Al distance increases by 0.16 Å. In that configuration, the angle $\alpha_{AuCO}$ is similar to those obtained in a previous work[15] for CO adsorption on top sites of free $Au_n$ clusters, which are in the range 162−173° for $n = 2-10$. For configuration b, adsorption of CO occurs at the interface of Au/$(Al_2O_3)_{20}$. The angle $\alpha_{CAuAl}$ is small enough to allow the CO molecule to bridge between the Au and the closest substrate oxygen atom. This process leads to a re-optimization of the substrate environment around an Au−Al bond, where the increase of the involved Al−O substrate distance by ∼0.15 Å is the more noticeable effect. For site c, the angle $\alpha_{CAuAl}$ is larger than for site b and smaller than for site a. This isomer configures another top-on-Au adsorption site, with CO more inclined toward the cluster than in isomer a. We also obtain the configuration for CO on the Au/(0001) surface, with a larger binding energy (∼0.75 eV). The different adsorption energy among the isomers $c_1$, $c_2$, and $c_3$ on the surface is due to the different orientation of the CO with respect to the surface (angles $\alpha_{AuCO}$ and $\alpha_{CAuAl}$ in Table 3). As long as the C−Au and C−O distances remain constant, the equilibrium $c_1$, $c_2$, and $c_3$ isomers suggest that CO rotates around the Au atom testing the more favorable sites of the underlying alumina surface.

Comparing the results obtained above for different alumina substrates, we notice that the Au/cluster system allows three different sites to adsorb CO, while the Au/(0001) surface offers only two sites, and in both systems, the binding energy is similar, about 1 eV or smaller. When CO is adsorbed in site a or c, the CO bond length is larger than the one calculated for the free molecule (1.16 Å), but it is still much larger when CO is adsorbed in site b. The bond length of CO in sites c (top) and b (bridge) maintains the same relation as for CO on top and bridge sites of $Au_n$ free clusters.[15] As we have shown in ref 15, "top" and "bridge" adsorption sites of CO on $Au_n$ can be distinguished by measuring the stretching frequency of CO. In Table 3, we see that the total excess electronic charge of CO is positive (more electrons) for site b and negative for top sites a and c, which is again similar to what is observed for bridge and top sites of CO adsorbed on free gold clusters.[15] Thus, we can anticipate a $\pi^*$ back-donation mechanism for the bonding of CO in bridge positions. Another clear distinction between sites b on one hand and c or a on the other hand is the larger C−Au bond distance in the bridge site than in the others. This should affect the infrared vibrational frequency, and spectroscopy could provide complementary information to that obtained by measuring the stretching frequency of CO absorbed on different sites of alumina substrates.

**TABLE 4: Properties of $Au_8$ Adsorbed on an $(Al_2O_3)_{20}$ Amorphouslike Cluster[a]**

| site | position | $E_{ads}$ (eV) | $d$ (Å) | α/α′[b] | $d_1/d_2$[c] | $\Delta Q_{Au}$(\|e\|) |
|---|---|---|---|---|---|---|
| 1 | Al(4) O(2) | 1.57 | 2.60−2.28 | 17.2° | 1.42 | 0.07 |
| 2 | O(2) O(3) | 1.07 | 2.39−2.35 | 2.0° | 1.05 | −0.11 |
| 3 | Al(4) Al(5) | 0.89 | 2.75−2.78 | 4.7° | 1.28 | −0.03 |
| 4 | Al(3) | 0.85 | 2.66 | (14.1°) | 1.10 | 0.19 |

[a] Different equilibrium configurations are denoted as in Figure 6. [b] The term α is the angle formed between the line that joins the two Au atoms closer to the $(Al_2O_3)_{20}$ cluster (atoms 1−3 in Figure 6b) and the two more distant atoms (atoms 4−6). When the $Au_8$ is in the on top position, α′ is the angle between the plane of the three Au atoms closer to the substrate (atoms 1− 2−7) and the plane formed by the central rhombus of $Au_8$ (atoms 2−7−5−8). [c] The fraction $d_1/d_2$ is the ratio between the rhombus diagonals.

**$Au_8$ Adsorption.** We study now the $Au_8$ cluster adsorption on an $(Al_2O_3)_{20}$ amorphouslike cluster. $Au_8$ is the smaller cluster which is active in the CO oxidation on Au/MgO.[4,5] We considered the minimum energy structure of $Au_8$ obtained in a previous work.[21] That isomer, shown in Figure 6, has a planar geometry.[22] During the relaxation of different initial $Au_8$/$(Al_2O_3)_{20}$ configurations, we fixed those atoms of $(Al_2O_3)_{20}$ more distant than the $Au_8$ cluster, which amounts to ∼20−30 atoms depending of the initial $Au_8$ position. These atoms are not affected by the gold atoms as we realized above for the Au adatom cases. In Table 4 is given the adsorption energy, bond distances of Au−substrate, geometry parameters, and excess charge (from Mulliken population analysis) on the $Au_8$ cluster, for the equilibrium structures of $Au_8$/$(Al_2O_3)_{20}$ complexes indicated in the left part of Figure 6.

In all adsorption sites that we considered, the Au−Au bond distances are larger than for the free $Au_8$ cluster. The gold cluster becomes deformed by the effect of the substrate and departs from planar geometry, because the Au atoms closer to the $(Al_2O_3)_{20}$ cluster move out of the plane of free $Au_8$. This result is quantified in Table 4 by means of the angles α, α′, and the $d_1/d_2$ ratio, whose values for the $Au_8$ free cluster are, 2.8°, 3.3°, and 1.06, respectively. The only exception is the second $Au_8$/$(Al_2O_3)_{20}$ isomer where the geometry of free $Au_8$ practically does not change. In this isomer, the gold cluster donates electron charge to the alumina cluster.

The energetically preferred adsorption sites of $Au_8$ on $(Al_2O_3)_{20}$ involve two low-coordinated Au atoms bonded to low coordinated atoms of the substrate, and the binding energy is higher when $Au_8$ binds two different element substrate atoms (Al and O).

**CO Adsorption on $Au_8$/$(Al_2O_3)_{20}$.** To study the CO adsorption on the higher binding energy isomer of the $Au_8$/$(Al_2O_3)_{20}$ complex, we considered different initial positions of CO and relaxed the positions of all atoms except those away from the gold cluster as in the section above. The higher adsorption energy isomers are presented in Figure 7 and Table 5. The CO molecule binds preferably (larger binding energy) on the gold atom which binds to an Al of the substrate. After CO adsorption, the Al−Au distance remains constant. In configuration 2, the CO binds to the 4-fold coordinated Au atom of the second row of $Au_8$ which is closer to the Au−Al bond. As a matter of fact, the Au−Al bond becomes broken (see Figure 7) for the CO/

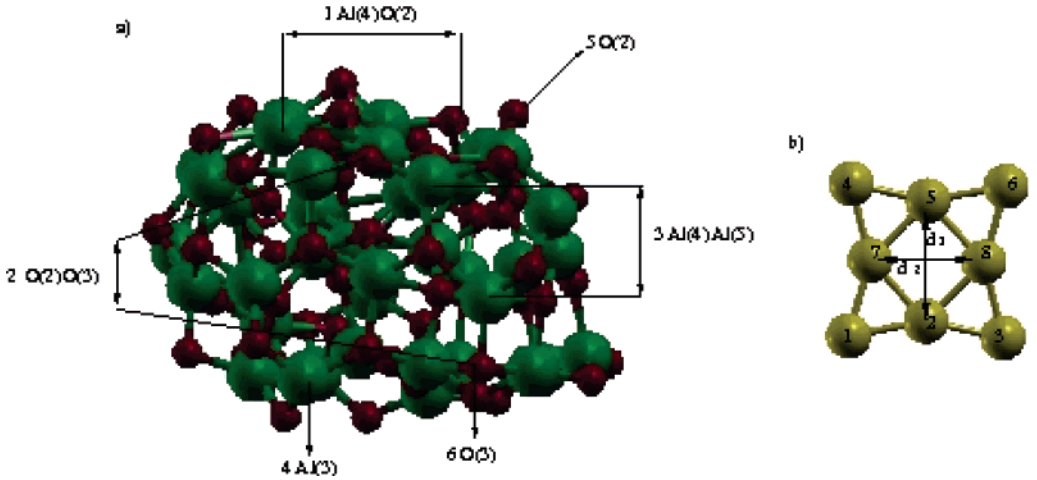


**Figure 6.** (a) Equilibrium geometry of $(Al_2O_3)_{20}$ showing the adsorption sites of $Au_8$, which are listed in Table 4 (with the coordination number of the substrate atom given in parentheses). (b) $Au_8$ cluster, in the gas phase, from ref 21.

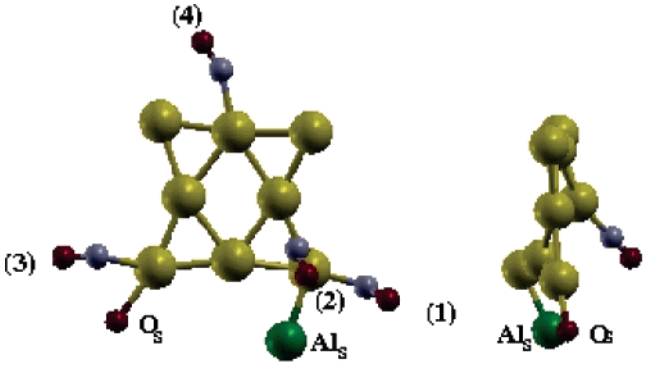


**Figure 7.** (a) Different equilibrium configurations for adsorption of CO on the more stable isomer of the $Au_8/(Al_2O_3)_{20}$ complex. The number in parentheses gives the order in decreasing binding energy. (b) Lateral view of isomer 2.

**TABLE 5: Properties of CO Adsorbed on an $Au_8/(Al_2O_3)_{20}$ Substrate**[a]

| | position | $E_{ads}$ (eV) | $d_{CO}$ (Å) | $d_{AuC}$ (Å) | $\alpha_{AuCO}$ | $\alpha$[b] | $\Delta Q_C$ | $\Delta Q_O$ |
|---|---|---|---|---|---|---|---|---|
| 1 | top | 0.62 | 1.17 | 2.08 | 144.9° | 15.8° | 0.13 | −0.20 |
| 2 | top | 0.59 | 1.16 | 2.20 | 177.9° | 21.2° | 0.11 | −0.28 |
| 3 | top | 0.49 | 1.16 | 2.02 | 173.1° | 15.8° | 0.07 | −0.20 |
| 4 | top | 0.46 | 1.17 | 2.08 | 152.0° | 18.8° | 0.13 | −0.20 |

[a] The first column identifies positions as in Figure 7. [b] The distortion angle $\alpha$ is defined in Table 4.

$Au_8/(Al_2O_3)_{20}$ isomers. For all configurations reported in Table 5, the CO molecule donates charge to the $Au_8/(Al_2O_3)_{20}$ complex, which is typical for CO adsorption on the top position of free gold clusters.[15]

The geometry of the $Au_8$/alumina for the isomer with larger CO binding energy does not change significantly after the CO adsorption. Nevertheless, for the other isomers, the alumina substrate does not change, but the Au rhombus is broken (position 2) or becomes more pronounced. On the other hand, the angle $\alpha$ suffers a more pronounced change with respect to the one of $Au_8/(Al_2O_3)_{20}$ (17.2°), when CO is absorbed in position 2. For that configuration, the alumina substrate atoms and the involved Au atoms move in opposite directions. One can guess that the energy barrier for this process will be higher than in the other cases.

Our more favorable (energetically) CO adsorption site is similar to the configuration obtained by Molina and Hammer[23] for $Au_n$ nanocrystals on MgO. The difference is that these authors obtained a greater inclination of CO toward the MgO substrate than the one we obtained for an alumina substrate.

From our results, we see that the loss of planarity of the free $Au_8$ after the CO adsorption is due, principally, to the alumina support and it is previous to the CO adsorption. Comparing our results with those of ref 15 for CO adsorption on free Au clusters, we can notice that in both cases CO is adsorbed on top of 2-fold coordinated Au atoms, resulting the same C−O bond distance and with the Au−C distance greater for the $Au_8/(Al_2O_3)_{20}$ complex (1.98 Å in the free gold cluster and 2.08 Å in the supported one). On the other hand, the second and fourth isomers of $CO/Au_8/(Al_2O_3)_{20}$ of Table 5 have no analogous counterpart for the free cluster, and this can be ascribed to a support effect. Therefore, the number of CO adsorption sites with not very different adsorption energy is greater for $Au_8$ supported on alumina than for the $Au_8$. Thus, though the CO binding energy of supported $Au_8$ is about half that for a free $Au_8$ cluster, the activity toward CO of the supported $Au_8$ cluster may be greater than for the free one.

## Summary and Conclusions

We have presented a theoretical study of CO adsorption on atomic Au and $Au_8$ clusters supported on two different alumina systems, namely, a $(Al_2O_3)_{20}$ amorphouslike cluster and the $\alpha$-$Al_2O_3$ (0001) surface. For both alumina systems, the energetically favorable adatom site is on top of a three-coordinated Al atom, the binding energy being higher for the alumina cluster than for the corundum surface. The adsorbed CO binds only to the Au adatom for both substrates, but after adsorption on the $Au/(Al_2O_3)_{20}$ cluster, the Au adatom forms a bridge between the Al and O of the alumina cluster. For $(Al_2O_3)_{20}$, we found different equilibrium adsorption sites than for the $\alpha$-$Al_2O_3$ surface. On the other hand, the $Au_8$ cluster binds through two atoms (Al and O) to the $(Al_2O_3)_{20}$ cluster and its structure changes from near planar to three-dimensional as an effect of the substrate. The more energetically favorable CO adsorption site is on top of a gold atom which is bonded to an Al atom of the alumina cluster. We do not find any CO bonding at bridge sites of the gold/alumina substrate. Comparing our results with the adsorption of CO on a free $Au_8$ cluster, we notice that in both cases the more energetically favorable adsorption site is on top of a gold atom and the interatomic CO distance is the same. However, we find new adsorption sites on the supported gold cluster. As long as the $Au_8$/(alumina-cluster) system allows more paths to adsorb CO than the free $Au_8$ cluster, one expects

a higher reactivity toward CO of the $Au_8/(Al_2O_3)_{20}$, despite the fact that the CO adsorption energy on a supported gold cluster is lower than for a free cluster.

**Acknowledgment.** We are grateful to MEC of Spain for the Grant Mat2005-03415 and for the financial support of FEDER from the European Community.

## References and Notes

(1) Haruta, H. *Catal. Today* **1997**, *36*, 153.
(2) Goodman, D. W. *Chem. Rev*. (Washington, D.C.) **1995**, *95*, 523. Gates, B. C. *Chem. Rev*. (Washington, D.C.) **1995**, *95*, 511.
(3) Yung, C. C.; Duh, J. G.; Huang, C. S. *Surf. Coat. Technol*. **2001**, *145*, 215.
(4) Sánchez, A.; Abbet, S.; Schneider, W.-D.; Heiz, U.; Häkkinen, H.; Barnett, R. N.; Landman, U. *J. Chem. Phys.* **1999**, *103*, 9573.
(5) Yoon, B.; Häkkinen, H.; Landman, U.; Wörz, A. S.; Antonietti, J.-M.; Abbet, S.; Judai, K.; Heiz, U. *Science* **2005**, *307*, 403.
(6) Wörz, A. S.; Heiz, U.; Cinquini, F.; Pachioni, G. *J. Phys. Chem. B* **2005**, *109*, 18418.
(7) Schübert, M. M.; Hackenberg, S.; Van Veen, A. C.; Mühler, M.; Plzak, V.; Behm, R. J. *J. Catal.* **2001**, *197*, 113.
(8) Comotti, M.; Li, W.-C.; Spliethoff, B.; Schüth, F. *J. Am. Chem. Soc*. **2006**, *128*, 917.
(9) Yan, W.; Mahurin, S. M.; Chen, B.; Pan, Z.; Overbury, H. *J. Phys. Chem. B* **2005**, *109*, *15489*.
(10) Cooper, V. R.; Kolpak, A. M.; Yourdshahayan, Y.; Rappe, A. M. *Phys. Rev. B* **2005**, *72*, 081409.
(11) Bäumer, M.; Freund, H.-J. *Prog. Surf. Sci.* **1999**, *61*, 127.
(12) Fu, L; Wu, N. Q.; Yang, J.; Qu, F.; Johnson, D. L.; Kung, M. C.; Dravid, V. P. *J. Phys. Chem. B* **2005**, *109*, 3704.
(13) Cruz-Hernández, N.; Fernández-Sanz, J. *Appl. Surf. Sci.* **2004**, *238*, 228.
(14) Feng, J.; Zhang, W.; Jiang, W. *Phys. Rev. B* **2005**, *72*, 115423.
(15) Fernández, E. M.; Ordejón, P.; Balbás, L. C. *Chem. Phys. Lett.* **2005**, *408*, 1277.
(16) Soler, J. M.; Artacho, E.; Gale, J. D.; García, A.; Junquera, J.; Ordejón, P.; Sánchez-Portal, D. *J. Phys: Condens. Matter*. **2002**, *14*, 2745; www.uam.es/siesta.
(17) Perdew, J. P.; Burke, K.; Ernzerhof, M. *Phys. Rev. Lett.* **1996**, *77*, 3865.
(18) Troullier, M.; Martins, J. L. *Phys. Rev. B* **1991**, *43*, 1993.
(19) Fernández, E. M.; Balbás, L. C. *Phys. Status Solidi B* **2005**, *203* (May issue).
(20) Fernández, E. M.; Borstel, G.; Soler, J. M.; Balbás, L. C. *Eur. Phys. J. D* **2003**, *24*, 245.
(21) Fernández, E. M.; Soler, J. M.; Garzón, I. L.; Balbás, L. C. *Phys. Rev. B* **2004**, *70*, 165403.
(22) Häkkinen, H.; Landman, U.; Yoon, B.; Li, X.; Zhai, H.-J.; Wang, L.-S. *J. Phys. Chem. A* **2003**, *107*, 6168.
(23) Molina, L. M.; Hammer, B. *Phys. Rev. B* **2003**, *69*, 155424.